

# QM/MM computational studies of substrate water binding to the oxygen-evolving centre of photosystem II

Eduardo M. Sproviero, Katherine Shinopoulos, José A. Gascón<sup>†</sup>,  
James P. McEvoy<sup>‡</sup>, Gary W. Brudvig and Victor S. Batista<sup>\*</sup>

*Department of Chemistry, Yale University, PO Box 208107, New Haven, CT 06520-8107, USA*

This paper reports computational studies of substrate water binding to the oxygen-evolving centre (OEC) of photosystem II (PSII), completely ligated by amino acid residues, water, hydroxide and chloride. The calculations are based on quantum mechanics/molecular mechanics hybrid models of the OEC of PSII, recently developed in conjunction with the X-ray crystal structure of PSII from the cyanobacterium *Thermosynechococcus elongatus*. The model OEC involves a cuboidal  $\text{Mn}_3\text{CaO}_4\text{Mn}$  metal cluster with three closely associated manganese ions linked to a single  $\mu_4$ -oxo-ligated Mn ion, often called the ‘dangling manganese’. Two water molecules bound to calcium and the dangling manganese are postulated to be substrate molecules, responsible for dioxygen formation. It is found that the energy barriers for the Mn(4)-bound water agree nicely with those of model complexes. However, the barriers for Ca-bound waters are substantially larger. Water binding is not simply correlated to the formal oxidation states of the metal centres but rather to their corresponding electrostatic potential atomic charges as modulated by charge-transfer interactions. The calculations of structural rearrangements during water exchange provide support for the experimental finding that the exchange rates with bulk  $^{18}\text{O}$ -labelled water should be smaller for water molecules coordinated to calcium than for water molecules attached to the dangling manganese. The models also predict that the  $\text{S}_1 \rightarrow \text{S}_2$  transition should produce opposite effects on the two water-exchange rates.

**Keywords:** oxomanganese complexes; photosystem II; oxygen evolution; photosynthesis; quantum mechanics/molecular mechanics; density functional theory

## 1. INTRODUCTION

The oxygen-evolving complex (OEC) of photosystem II (PSII) is a high-valent manganese- and calcium-containing cofactor that catalyses water cleavage to dioxygen according to the so-called ‘S-state’ catalytic cycle (figure 1), proposed by Joliot & Kok (Joliot *et al.* 1969; Kok *et al.* 1970). Substrate water molecules responsible for  $\text{O}_2$  formation are thought to ligate to metal ions in the OEC early in the catalytic cycle, as suggested by pulsed electron paramagnetic resonance (EPR) spectroscopy (Britt *et al.* 2004; Evans *et al.* 2004), near infrared Raman spectroscopy (Cua *et al.* 2000) and Fourier transform infrared spectroscopy (Noguchi & Sugiura 2002; Kimura *et al.* 2005). This paper analyses the specific water-binding sites and the effect of oxidation of the OEC on substrate water binding, which remain controversial.

A direct scrutiny of substrate water molecules by time-resolved mass spectrometry (MS) has determined

different exchange rates ( $k_{\text{ex}}$ ) with bulk  $^{18}\text{O}$ -labelled water of the two substrate water molecules of the OEC in the  $\text{S}_0$ ,  $\text{S}_1$ ,  $\text{S}_2$  and  $\text{S}_3$  states (Hillier & Wydrzynski 2000, 2001, 2004). The more slowly exchanging water ( $\text{W}^{\text{slow}}$ ) was found to be associated with  $\text{Ca}^{2+}$ , implying that the fast-exchanging water ( $\text{W}^{\text{fast}}$ ) must be bound to a manganese ion. This is rather surprising since manganese ions are thought to be higher valent (e.g.  $\text{Mn}^{3+}$  or  $\text{Mn}^{4+}$ ) than  $\text{Ca}^{2+}$  in the OEC. In addition, it has been observed that the exchange rate of  $\text{W}^{\text{slow}}$  ( $k_{\text{ex}}^{\text{slow}}$ ) increases by two orders of magnitude upon  $\text{S}_1 \rightarrow \text{S}_2$  oxidation, with  $k_{\text{ex}}(\text{S}_1) = 0.02 \text{ s}^{-1}$  and  $k_{\text{ex}}(\text{S}_2) = 2.0 \text{ s}^{-1}$  (Hendry & Wydrzynski 2003; Hillier & Wydrzynski 2004). These exchange rates correspond to activation energies of approximately 20 and 17  $\text{kcal mol}^{-1}$  in the  $\text{S}_1$  and  $\text{S}_2$  states, respectively. Considering that the  $\text{S}_1 \rightarrow \text{S}_2$  transition involves oxidation of a manganese centre, the observed acceleration of the exchange of  $\text{W}^{\text{slow}}$  is also intriguing since it implies that the oxidation of a manganese centre must indirectly affect the exchange rate of a calcium-bound water molecule. While these observations are reproducible and unambiguous, it is not clear whether they can be rationalized by previously proposed mechanistic models (Pecoraro *et al.* 1998; Vrettos *et al.* 2001; Messinger 2004). The calculations reported in this paper address both of these

\* Author for correspondence (victor.batista@yale.edu).

<sup>†</sup> Present address: Department of Chemistry, University of Connecticut, Unit 3060, Storrs, CT 06269, USA.

<sup>‡</sup> Present address: Department of Chemistry, Regis University, 3333 Regis Boulevard, Denver, CO 80221, USA.

One contribution of 20 to a Discussion Meeting Issue ‘Revealing how nature uses sunlight to split water’.

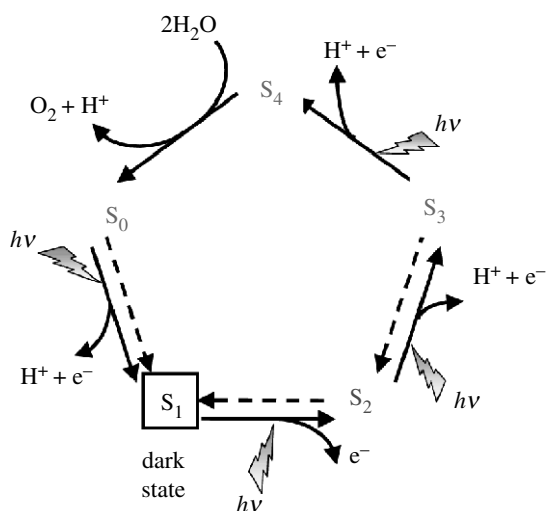


Figure 1. Catalytic cycle proposed by Joliot *et al.* (1969) and Kok *et al.* (1970) for water splitting into dioxygen, protons and electrons at the OEC in PSII. Solid arrows indicate light-driven reactions and dashed arrows indicate dark reactions.

observations through the analysis of structural models of the OEC in the  $S_1$  and  $S_2$  states (Sproviero *et al.* 2006a,b, 2007).

The computational models are constructed using state-of-the-art quantum mechanics/molecular mechanics (QM/MM) hybrid methods, with QM layers described by the density functional theory (DFT) with the Becke-3-Lee-Yang-Parr (B3LYP) hybrid density functional, in conjunction with the X-ray crystal structure of PSII from the cyanobacterium *Thermosynechococcus elongatus* (Ferreira *et al.* 2004). This work builds upon recent studies where the capabilities and limitations of the B3LYP functional were investigated as applied to the studies of structural and electronic properties of high-valent multinuclear oxomanganese complexes (Sproviero *et al.* 2006a,b, 2007).

The computational models involve coordination of substrate water molecules as terminal ligands, in agreement with earlier proposals (Hoganson & Babcock 1997; Haumann & Junge 1999; Schlodder & Witt 1999; McEvoy & Brudvig 2004; Messinger 2004; McEvoy *et al.* 2005a,b; Sproviero *et al.* 2006a), but in contrast to other suggested models that involve coordination as oxo-bridges between Mn ions (Brudvig & Crabtree 1986; Pecoraro *et al.* 1994; Yachandra *et al.* 1996; Nugent *et al.* 2001; Robblee *et al.* 2001; Messinger 2004). The reported computations address general aspects of water exchange as well as the underlying mechanisms of water exchange for the OEC of PSII in the  $S_1$  and  $S_2$  states. The calculations thus complement earlier studies of water exchange in transition metal complexes (Rotzinger 1997; Helm & Merbach 1999; Rotzinger 2005; Cady *et al.* 2006; Houston *et al.* 2006; Tagore *et al.* 2006, 2007), including theoretical studies of manganese complexes, based on Hartree-Fock and complete active-space self-consistent field theories (Rotzinger 1997, 2005; Tsutsui *et al.* 1999; Lundberg *et al.* 2003) as well as DFT studies of water exchange in other transition metal complexes (Deeth & Elding 1996; Hartmann *et al.* 1997, 1999; Vallet *et al.* 2001; Lundberg *et al.* 2003).

## 2. DFT-QM/MM MODELLING

The QM/MM methodology involves the two-layer ONIOM electronic-embedding (EE) approach (Dapprich *et al.* 1999), as implemented in GAUSSIAN v. 03 (Frisch *et al.* 2004), combined with high-quality initial states for the ligated OEC metal cluster that were obtained using ligand field theory (Vacek *et al.* 1999) as implemented in JAGUAR v. 5.5 (Schrodinger 2004). The combined approach exploits the high efficiency of ligand field theory for definitions of specific initial-guess spin-electronic states, the flexible definitions of QM layers according to the link-hydrogen atom scheme and the possibility of modelling open-shell systems by performing unrestricted DFT (e.g. UB3LYP) calculations.

The study of transition metal compounds has been dominated by the well-established B3LYP functional. However, the estimated error of the B3LYP treatment of water-exchange energy barriers is approximately 2–3 kcal mol<sup>-1</sup> (Helm & Merbach 1999; Lundberg *et al.* 2003). Unfortunately, this error is comparable to the observed changes of activation energies induced by oxidation of the OEC. Therefore, quantitative calculations of activation energy barriers are still beyond the capabilities of DFT. The reported studies are thus focused on the qualitative and semiquantitative analysis of general aspects of substrate water-exchange mechanism as determined by the nature of the metal cluster and the effect of electrostatic interactions with the surrounding protein environment.

The QM layer includes the following: the Mn<sub>3</sub>-CaO<sub>4</sub>Mn complex; the directly ligating carboxylate groups of D1-E189, CP43-E354, D1-A344, D1-E333, D1-D170, D1-D342 and the imidazole ring of D1-H332; and bound water molecules, hydroxide and chloride ions. The QM layer thus includes all species in the first coordination shell of metal centres as well as the exchanging water molecule W\* (figure 2). The rest of the system defines the MM layer. The boundaries between QM and MM layers are defined for the corresponding amino acid residues (i.e. D1-E189, CP43-E354, D1-A344, D1-E333, D1-D170, D1-D342 and D1-H332) by completing the covalency of frontier atoms according to the standard link-hydrogen atom scheme.

The total energy  $E$  of the system is computed as follows:

$$E = E^{\text{MM,full}} + E^{\text{QM,red}} - E^{\text{MM,red}} \quad (2.1)$$

where  $E^{\text{MM,full}}$  is the energy of the complete system as described by the Amber MM force field, while  $E^{\text{QM,red}}$  and  $E^{\text{MM,red}}$  are the energies of the reduced system computed at the QM and MM levels of theory, respectively. Electrostatic interactions between the reduced system and the surroundings are included in the evaluation of  $E^{\text{QM,red}}$  and  $E^{\text{MM,red}}$  at the QM and MM levels, respectively. Therefore, the resulting QM/MM evaluation of the total energy  $E$  involves a quantum mechanical description of polarization of the reduced system due to the electrostatic influence of the surrounding protein environment. In addition, the polarization of the protein environment, usually neglected in standard QM/MM calculations, is modelled according to the self-consistent 'Moving Domain-QM/MM' (MoD-QM/MM) approach (Gascon *et al.* 2006).

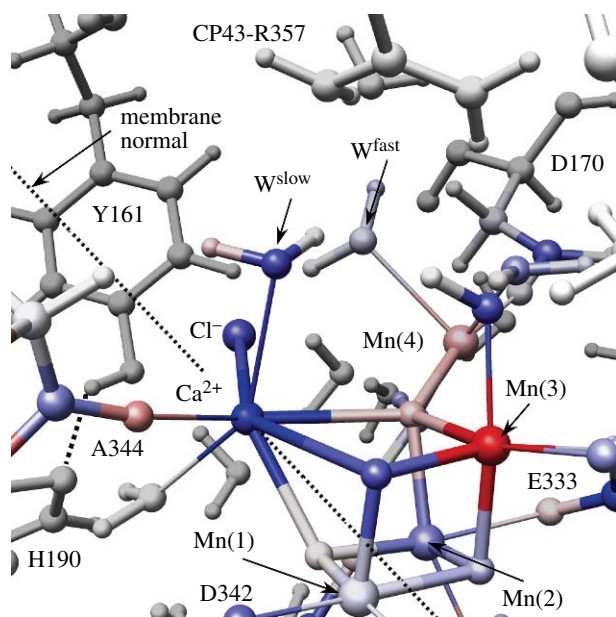


Figure 2. DFT-QM/MM structural model of the OEC of PSII (Sproviero *et al.* 2006a). Fast- and slow-exchanging substrate water molecules,  $W^{\text{fast}}$  and  $W^{\text{slow}}$ , are coordinated to Mn(4) and  $\text{Ca}^{2+}$ , respectively. Red (blue) colours indicate an increase (decrease) in ESP atomic charges due to  $S_1 \rightarrow S_2$  oxidation. Bright colours indicate changes of approximately 15–20% (table 1). All amino acid residues correspond to the D1 protein subunit, unless otherwise indicated.

Fully relaxed QM/MM molecular structures for the analysis of minimum energy paths (MEPs) for water detachment and exchange are obtained at the ONIOM-EE (UHF B3LYP/lacvp,6-31G(2df),6-31G:AMBER) level of theory by geometry optimization of the complete structural models. A combination of basis sets is applied in order to optimize the efficiency of QM/MM calculations, including the LACVP basis set for Mn ions that considers the non-relativistic electron core potentials (ECPs), the 6-31G(2df) basis set for bridging  $\text{O}^{2-}$  ions that includes polarization functions on  $\mu$ -oxo bridging oxides and the 6-31G basis set for the rest of the atoms in the QM layer. Such a combination of basis sets has been validated through extensive benchmark calculations on high-valent manganese complexes (Sproviero *et al.* 2006a,b).

### 3. STRUCTURAL MODELS OF THE $\text{O}_2$ -EVOLVING CENTRE

The QM/MM hybrid models of the OEC in PSII suggest that the two substrate water molecules can bind to  $\text{Ca}^{2+}$  and Mn(4) on the ‘active face’ of the OEC (Sproviero *et al.* 2006a), consistent with the previously proposed mechanistic hypothesis (Pecoraro *et al.* 1998; Vrettos *et al.* 2001; McEvoy *et al.* 2005b; figure 2). Two redox states of comparable energies are predicted: model (a) where the dangling manganese Mn(4) is pentacoordinated and the oxidation states are  $\text{Mn}_4(\text{IV}, \text{IV}, \text{III}, \text{III})$  (i.e. Mn(1)=IV, Mn(2)=IV, Mn(3)=III, Mn(4)=III) and model (b) where an additional water ligand is completing the hexacoordinated shell of Mn(4) and the oxidation states are  $\text{Mn}_4(\text{IV}, \text{III}, \text{III}, \text{IV})$ . These results are partially consistent with EPR and X-ray spectroscopic evidence (Ono

Table 1. ESP charges, spin population and formal oxidation numbers of metal centres and substrate water molecules in DFT-QM/MM models of the OEC of PSII, introduced in the text, in the  $S_1$  and  $S_2$  states.

centre	ESP charge		spin pop. (oxid. no.)	
	$S_1$	$S_2$	$S_1$	$S_2$
Mn(4)	+1.35	+1.49	−3.80 (+3)	+3.79 (+3)
Mn(3)	+1.26	+1.59	+3.82 (+3)	−2.74 (+4)
$\text{Ca}^{2+}$	+1.77	+1.56	+0.01 (+2)	0.00 (+2)
$\text{O}(W^{\text{slow}})^{\text{a}}$	−0.82	−0.96	−0.00 (−2)	+0.00 (−2)
$\text{O}(W^{\text{fast}})^{\text{b}}$	−0.90	−0.88	−0.05 (−2)	+0.06 (−2)

<sup>a</sup>Oxygen of  $W^{\text{slow}}$  ligated to  $\text{Ca}^{2+}$ .

<sup>b</sup>Oxygen of  $W^{\text{fast}}$  ligated to Mn(4).

*et al.* 1992; Yachandra *et al.* 1993; Roelofs *et al.* 1996; Bergmann *et al.* 1998; Iuzzolino *et al.* 1998; Dau *et al.* 2001; Messinger *et al.* 2001) but disagree with the suggested low-valent  $\text{Mn}_4(\text{III}, \text{III}, \text{III}, \text{III})$  state (Zheng & Dismukes 1996; Kuzek & Pace 2001).

In contrast to the incomplete ligation scheme suggested by the X-ray model structures, the QM/MM models involve metal ions with the usual number of ligands (i.e. five and six ligands coordinated to Mn ions with oxidation states III and IV, respectively, and seven to eight ligands attached to  $\text{Ca}^{2+}$ , which usually finds six to eight ligands). The proteinaceous ligation includes the following:  $\eta^2$ -coordination of E333 to both Mn(3) and Mn(2) and hydrogen bonding to the protonated CP43-E354 (neutral state) residue; monodentate coordination of D342, CP43-E354 and D170 to Mn(1), Mn(3) and Mn(4), respectively; and ligation of E189 and H332 to Mn(2). The relative stability of the two redox states is determined by the strained coordination of H332 to the Mn cluster. The hexacoordinated Mn(2) stabilizes the oxidation state IV when Mn(4) is pentacoordinated, and the oxidation state III (with a Jahn–Teller elongation along the Mn–H332 axis) when the coordination sphere of Mn(4) is complete.

Both the redox isomers of the OEC of PSII are neutral in the  $S_1$  state and predict anti-ferromagnetic coupling between Mn(1) and Mn(2), Mn(2) and Mn(3), and Mn(3) and Mn(4), but frustrated spin coupling between Mn(1) and Mn(3) in the cuboidal structure. Table 1 presents the DFT-QM/MM analysis of distribution spin populations and charge in the metal centres of the OEC model (a).

### 4. WATER BINDING TO THE $\text{O}_2$ -EVOLVING CENTRE

The QM/MM structural models, introduced in §3, allow for the evaluation of specific metal–water interactions and the potential energy profiles associated with the MEPs for water detachment and exchange. The MEPs are found by energy minimization with respect to nuclear and electronic coordinates, while progressively detaching substrate water molecules from their corresponding coordination metal centres. The resulting structural rearrangements provide an insight on the water-exchange mechanisms and the relative binding strengths since elongation of the metal–oxygen

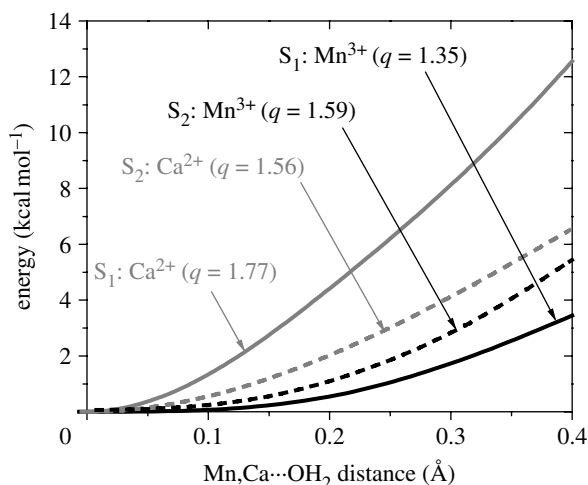


Figure 3. DFT-QM/MM energy profiles as a function of the coordination bond lengths between substrate water molecules attached to  $\text{Ca}^{2+}$  (grey lines) and the dangling  $\text{Mn}^{3+}$  (black lines), for the OEC of PSII in the  $S_1$  (dashed lines) and  $S_2$  (solid lines) states. ESP ionic charges are indicated in parenthesis ( $q$ ). The energy barriers are 19.3, 16.6, 8.4 and 7.9 kcal mol $^{-1}$  for water exchange from  $\text{Ca}^{2+}(S_1)$ ,  $\text{Ca}^{2+}(S_2)$ ,  $\text{Mn}^{3+}(S_2)$  and  $\text{Mn}^{3+}(S_1)$ , respectively.

bond is the primary step in water exchange and presumably rate determining in this case (Rotzinger 1997; Lundberg *et al.* 2003; Rotzinger 2005).

Figure 3 shows the resulting energy profiles for the MEPs, while progressively detaching substrate water molecules from  $\text{Ca}^{2+}$  and the dangling manganese for the OEC in the  $S_1$  and  $S_2$  states  $\text{Mn}_4(\text{IV},\text{IV},\text{III},\text{III})$  and  $\text{Mn}_4(\text{IV},\text{IV},\text{IV},\text{III})$ , respectively. It is shown that stretching the  $\text{Ca}^{2+}-\text{W}^{\text{slow}}$  bond is energetically more demanding than stretching the  $\text{Mn}(4)-\text{W}^{\text{fast}}$  bond of the OEC in both the  $S_1$  and the  $S_2$  states. Furthermore, figure 3 shows that advancing the OEC from the  $S_1$  to the  $S_2$  state weakens the  $\text{Ca}^{2+}-\text{W}^{\text{slow}}$  bond and strengthens the coordination of  $\text{W}^{\text{fast}}$  to  $\text{Mn}(4)$ . This is due to the underlying redistribution of charge in the complex induced by the  $S_1 \rightarrow S_2$  transition. Analogous results are obtained for the redox isomers of the  $S_1$  and  $S_2$  states with oxidation numbers  $\text{Mn}_4(\text{IV},\text{III},\text{III},\text{IV})$  and  $\text{Mn}_4(\text{IV},\text{IV},\text{III},\text{IV})$ , respectively.

The results reported in figure 3 are consistent with the experimental observation that  $\text{W}^{\text{slow}}$  is bound to  $\text{Ca}^{2+}$ , implying that  $\text{W}^{\text{fast}}$  is attached to a high-valent manganese ion, even when the formal oxidation number of  $\text{Ca}^{2+}$  is +2 and the oxidation numbers of  $\text{Mn}(4)$  are +3 and +4 in redox isomers (a) and (b), respectively. These results can be rationalized by noting that charge transfer between manganese ions and ligand/oxo-bridges affects the net ionic charges of metal centres, complicating the correlation with formal oxidation numbers (Sproviero *et al.* 2006a,b, 2007). The underlying charge-transfer delocalization process is common to synthetic oxomanganese complexes (Sproviero *et al.* 2006b) and partially neutralizes the net ionic charges of the metal centres, leaving a smaller positive charge on  $\text{Mn}(4)$  ( $q = +1.35$ ) than on  $\text{Ca}^{2+}$  ( $q = +1.77$ ; table 1). Therefore, it is not surprising that  $\text{W}^{\text{slow}}$  is attached to  $\text{Ca}^{2+}$ , as indicated by the energetic analysis of figure 3, even when such a metal centre has a smaller oxidation number than  $\text{Mn}(4)$ .

The computational results reported in figure 3 and table 1 are also consistent with the experimental observation that  $k_{\text{ex}}^{\text{slow}}$  increases and  $k_{\text{ex}}^{\text{fast}}$  decreases upon  $S_1 \rightarrow S_2$  oxidation (Hillier & Wydrzynski 2004). These opposite changes in the two water-exchange rates, induced by the  $S_1 \rightarrow S_2$  transition, can also be traced to the corresponding changes in ESP ionic charges modulated by charge-transfer interactions. Table 1 shows that the redistribution of charge, induced by the  $S_1 \rightarrow S_2$  oxidation, decreases the ionic charge of calcium ( $\Delta q = -0.21$ ) and increases the ionic charge of  $\text{Mn}(4)$  ( $\Delta q = +0.24$ ). This is consistent with the energetic analysis predicting that  $S_1 \rightarrow S_2$  oxidation weakens the  $\text{Ca}^{2+}-\text{W}^{\text{slow}}$  bond and strengthens the coordination of  $\text{W}^{\text{fast}}$  to  $\text{Mn}(4)$ .

In order to analyse the origin of the underlying redistribution of electronic density, we note that the oxomanganese complex is neutral in the  $S_1$  resting state, as described by the DFT-QM/MM models. Upon  $S_1 \rightarrow S_2$  oxidation, however, the complex becomes positively charged, strengthening the electrostatic interactions with negatively charged ligands. In particular,  $\text{Ca}^{2+}$  and D1-A344 are paired up by charge-transfer interactions, and most of the electronic density acquired by  $\text{Ca}^{2+}$  upon  $S_1 \rightarrow S_2$  oxidation ( $\Delta q = -0.21$ ) is transferred from the ligated carboxylate group of D1-A344 (the corresponding change in the ESP atomic charge of the ligated oxygen atom of D1-A344 is  $\Delta q = +0.2$ ). These results indicate that charge-transfer interactions are strongly modulated by the oxidation state of the oxomanganese complex, indirectly regulating substrate water binding to the metal cluster.

In addition to the ESP approach, various other methods are available for the analysis of partial atomic charges, yielding slightly different quantitative results. However, the methods consistently predict that: (i) the atomic charges of  $\text{Ca}^{2+}$ ,  $\text{Mn}^{3+}$  and  $\text{Mn}^{4+}$  in the OEC are always smaller than their corresponding formal charges, due to charge-transfer interactions with coordinated counterions, (ii) the reduction of atomic charges is more significant for high-valent manganese ions  $\text{Mn}^{3+}$  and  $\text{Mn}^{4+}$  than for  $\text{Ca}^{2+}$ , and (iii) the charge of  $\text{Ca}^{2+}$  is further neutralized upon  $S_1 \rightarrow S_2$  oxidation by charge transfer with the carboxylate ligand of D1-A344.

Considering that the  $\text{Mn}_3\text{CaO}_4\text{Mn}$  metal cluster involves carboxylate groups ligated to  $\text{Ca}^{2+}$  as well as carboxylate ligands coordinated to  $\text{Mn}^{3+}$  and  $\text{Mn}^{4+}$  ions, it is important to address the origin of the preferential charge transfer between D1-A344 and  $\text{Ca}^{2+}$  upon  $S_1 \rightarrow S_2$  oxidation of the OEC. To this end, we have performed a bond-order analysis, based on natural atomic orbitals (Reed *et al.* 1988). The results indicate that  $\text{Mn}-\text{O}$  bonds are predominantly covalent dative (Wiberg bond index = 1.05) while the  $\text{Ca}-\text{O}$  bonds are ionic (Wiberg bond index = 0.32). The difference is mainly due to charge delocalization from the p-orbitals of the oxo-ligands to vacant d-orbitals in manganese. Further, it is found that the delocalization mechanism involves both alpha and beta orbitals in similar amounts. Therefore, the total charges of the manganese ions are significantly reduced while the number of unpaired electrons (i.e. the oxidation state) remains almost unchanged. Therefore, the

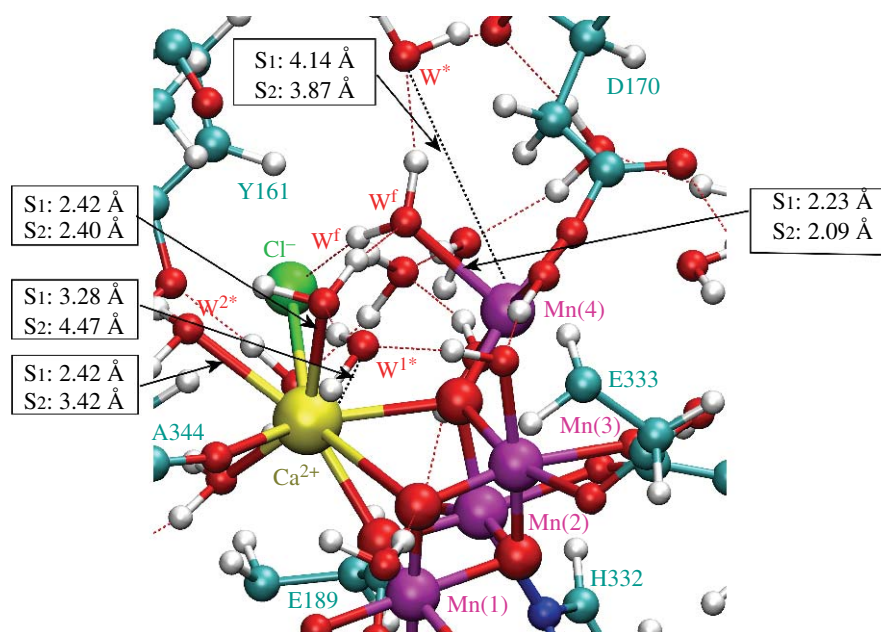


Figure 4. Structural model of the OEC of PSII in the  $S_1$  and  $S_2$  states. Ligated and exchanging water molecules are labelled  $W^s$  ( $W^{\text{slow}}$ ),  $W^f$  ( $W^{\text{fast}}$ ) and  $W^*$ , respectively. All amino acid residues correspond to the D1 protein subunit, unless otherwise indicated.

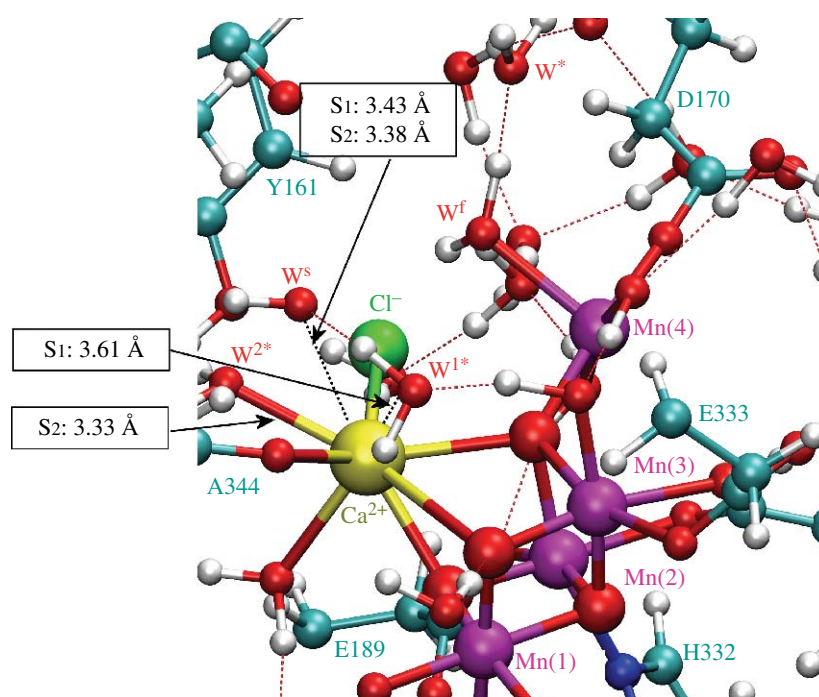


Figure 5. Structural model of the OEC of PSII in the  $S_1$  and  $S_2$  states at the transition state configurations for water exchange from  $\text{Ca}^{2+}$ . The water-exchange energy barriers in the  $S_1$  and  $S_2$  states are 19.3 and 16.6 kcal mol $^{-1}$ , respectively. Substrate and exchanging water molecules are labelled  $W^s$  ( $W^{\text{slow}}$ ) and  $W1^*$ , respectively. All amino acid residues correspond to the D1 protein subunit, unless otherwise indicated.

underlying charge delocalization between manganese and oxo-bridges indirectly affects the relative strengths of charge-transfer interactions between metal centres and carboxylate ligands.

Figures 4–6 show the initial and TS configurations along the MEPs for water exchange from  $\text{Ca}^{2+}$  and Mn(4), as described by the DFT-QM/MM structural models of the OEC, including a detailed description of coordination bond lengths. In the initial states (figure 4), substrate water molecules are attached to the metal centres forming hydrogen bonds with the

exchanging water molecules. In the TS configurations (figures 5 and 6), the coordination bonds of the substrate water molecules are stretched and the substituting water molecules are displaced relative to their initial positions. Further displacement beyond the transition state induces coordination of the exchanging water molecules. This structural analysis indicates that the exchange mechanism involves concerted interchange with dissociative character (i.e. without formation of any intermediate state of lower or higher coordination number).

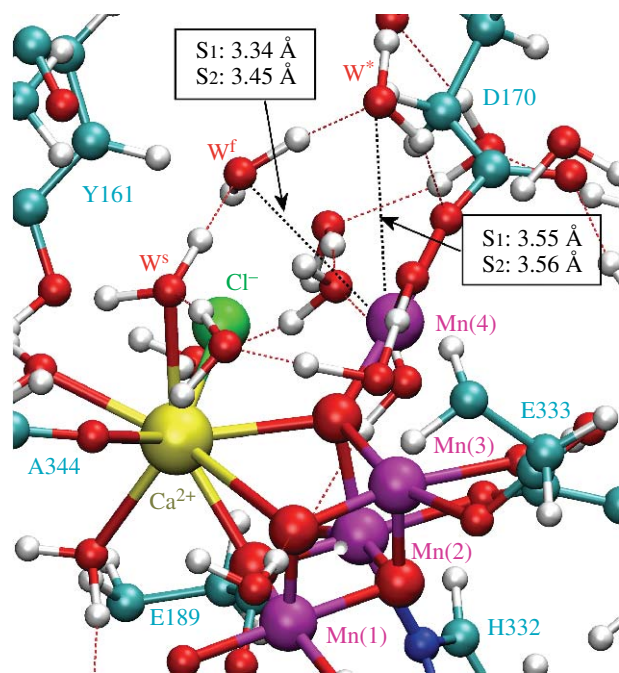


Figure 6. Structural model of the OEC of PSII in the  $S_1$  and  $S_2$  states at the transition state configurations for water exchange from Mn(4). The water-exchange energy barriers in the  $S_1$  and  $S_2$  states are 7.9 and 8.4 kcal mol<sup>-1</sup>, respectively. Substrate and exchanging water molecules are labelled  $W^f$  ( $W^{\text{fast}}$ ) and  $W^*$ , respectively. All amino acid residues correspond to the D1 protein subunit, unless otherwise indicated.

The comparison of the coordination bond lengths of exchanging water molecules in the TS configurations indicates that water exchange from  $\text{Ca}^{2+}$  gains a more dissociative character upon  $S_1 \rightarrow S_2$  oxidation of the OEC (i.e. the TS coordination bonds are more stretched in the  $S_2$  state). This is probably due to the reduction in the atomic charge of  $\text{Ca}^{2+}$  induced by charge-transfer interactions with D1-A344. The dissociative character is also observed for water exchange from the dangling manganese in both the  $S_1$  and the  $S_2$  states, probably due to the reduced charge of manganese induced by charge delocalization between manganese and oxo-bridges.

The calculated DFT-QM/MM energy barriers for water exchange from Mn(4) are 7.9 and 8.4 kcal mol<sup>-1</sup> in the  $S_1$  and  $S_2$  states, respectively. These are comparable to the barriers in hydrated Mn complexes, such as  $[(\text{H}_2\text{O})_2(\text{OH})_2\text{Mn}^{\text{IV}}(\mu\text{-O})_2\text{Mn}^{\text{IV}}(\text{H}_2\text{O})_2(\text{OH})_2]$  and  $[\text{Mn}^{\text{IV}}(\text{H}_2\text{O})_2(\text{OH})_4]$ , where the exchange of terminal water ligands requires 8.6–9.6 kcal mol<sup>-1</sup> (Tsutsui *et al.* 1999; Lundberg *et al.* 2003). In contrast, the DFT-QM/MM energy barriers for water exchange from  $\text{Ca}^{2+}$  are 19.3 and 16.6 kcal mol<sup>-1</sup> for the OEC in the  $S_1$  and  $S_2$  states, respectively. The higher energy barriers are determined by the nature of the interactions in the hydrophobic OEC-binding pocket. The exchanging water molecules have incomplete solvation shells and therefore make only two to three hydrogen bonds with the surrounding molecules or ions. Such an incomplete structure of hydrogen bonds stabilizes the coordination of water molecules to the metal cluster and strongly correlates the orientation and displacement of the exchanging water molecules.

These findings suggest that the molecular environment surrounding the OEC of PSII has been highly optimized by natural selection to stabilize the attachment of substrate water molecules to metal centres, correlating their orientations and displacements and reducing the interactions with surrounding amino acid residues. At the same time, the hydrophobic environment stabilizes the coordination of  $\text{Cl}^-$  to the ionic cluster as well as the coordination of the oxomanganese cluster to carboxylate groups of proteinaceous ligands.

## 5. CONCLUDING REMARKS

The computational analysis of water binding in complete DFT-QM/MM structural models of the OEC in PSII indicates that the barriers for exchange of Mn(4)-bound water agree nicely with those of model complexes. However, the barriers for Ca-bound waters are substantially larger. The calculations also provide theoretical support to the surprising experimental finding that the slow-exchanging substrate water of the OEC is associated with calcium, implying that the fast-exchanging substrate water is coordinated with manganese. Furthermore, the DFT-QM/MM models provide a rationale for the opposing effects of the  $S_1 \rightarrow S_2$  transition on the two rate constants. It is concluded that the mechanism and energetics of water binding to metal centres in the OEC is not simply correlated to the formal oxidation states of the metal ions but rather to their corresponding partial ionic charges, as modulated by charge-transfer interactions with coordinated ligands. The reported findings help to rationalize experimental results probing substrate water molecules in the water-splitting chemistry of PSII, providing fundamental insight into the electronic structure of the OEC and the surrounding protein environment.

V.S.B. acknowledges supercomputer time from the National Energy Research Scientific Computing (NERSC) center and financial support from Research Corporation, Research Innovation Award no. RI0702, a Petroleum Research Fund Award from the American Chemical Society PRF no. 37789-G6, the National Science Foundation (NSF) Career Program Award CHE no. 0345984, the Alfred P. Sloan Fellowship and the Camille Dreyfus Teacher-Scholar Award. G.W.B. acknowledges support from the National Institutes of Health, grant GM32715.

## REFERENCES

- Bergmann, U. *et al.* 1998 Characterization of the Mn oxidation states in photosystem II by  $\text{K}^\beta$  X-ray fluorescence spectroscopy. *J. Phys. Chem. B* **102**, 8350–8352. (doi:10.1021/jp982038s)
- Britt, R. D., Campbell, K. A., Peloquin, J. M., Gilchrist, M. L., Aznar, C. P., Dicus, M. M., Robblee, J. & Messinger, J. 2004 Recent pulsed EPR studies of the photosystem II oxygen-evolving complex: implications as to water oxidation mechanisms. *Biochim. Biophys. Acta* **1655**, 158–171. (doi:10.1016/j.bbabi.2003.11.009)
- Brudvig, G. W. & Crabtree, R. H. 1986 Mechanism for photosynthetic  $\text{O}_2$  evolution. *Proc. Natl Acad. Sci. USA* **83**, 4586–4588. (doi:10.1073/pnas.83.13.4586)
- Cady, C. W., Incarvito, C., Brudvig, G. W. & Crabtree, R. H. 2006 Secondary bonding in a six-coordinate Mn(II) complex as a model of associative substitution. *Inorg. Chim. Acta* **359**, 2509–2512. (doi:10.1016/j.ica.2006.02.005)

- Cua, A., Stewart, D. H., Reifler, M. J., Brudvig, G. W. & Bocian, D. F. 2000 Low-frequency resonance Raman characterization of the oxygen-evolving complex of photosystem II. *J. Am. Chem. Soc.* **122**, 2069–2077. (doi:10.1021/ja9932885)
- Dapprich, S., Komaroni, I., Byun, K. S., Morokuma, K. & Frisch, M. J. 1999 A new ONIOM implementation in Gaussian98. Part I. The calculation of energies, gradients, vibrational frequencies and electric field derivatives. *Theochem* **461**, 1–21. (doi:10.1016/S0166-1280(98)00475-8)
- Dau, H., Iuzzolino, L. & Dittmer, J. 2001 The tetra-manganese complex during its redox cycle—X-ray absorption results and mechanistic implications. *Biochim. Biophys. Acta* **1503**, 24–39. (doi:10.1016/S0005-2728(00)00230-9)
- Deeth, R. J. & Elding, L. I. 1996 Theoretical modeling of water exchange on  $[\text{Pd}(\text{H}_2\text{O})_4]^{2+}$ ,  $[\text{Pt}(\text{H}_2\text{O})_4]^{2+}$ , and *trans*- $[\text{PtCl}_2(\text{H}_2\text{O})_2]$ . *Inorg. Chem.* **35**, 5019–5026. (doi:10.1021/ic950335v)
- Evans, M. C. W., Nugent, J. H. A., Ball, R. J., Muhiuddin, I. & Pace, R. J. 2004 Evidence for a direct manganese–oxygen ligand in water binding to the  $\text{S}_2$  state of the photosynthetic water oxidation complex. *Biochemistry* **43**, 989–994. (doi:10.1021/bi035489y)
- Ferreira, K. N., Iverson, T. M., Maghlaoui, K., Barber, J. & Iwata, S. 2004 Architecture of the photosynthetic oxygen-evolving center. *Science* **303**, 1831–1838. (doi:10.1126/science.1093087)
- Frisch, M. J. et al. 2004 *Gaussian 03. Revision C.02*. Wallingford, CT: Gaussian, Inc.
- Gascon, J. A., Leung, S. S. F., Batista, E. R. & Batista, V. S. 2006 A self-consistent space-domain decomposition method for QM/MM computations of protein electrostatic potentials. *J. Chem. Theor. Comput.* **2**, 175–186. (doi:10.1021/ct050218h)
- Hartmann, M., Clark, T. & van Eldik, R. 1997 Hydration and water exchange of Zinc(II) ions. Application of density functional theory. *J. Am. Chem. Soc.* **119**, 7843–7850. (doi:10.1021/ja970483f)
- Hartmann, M., Clark, T. & van Eldik, R. 1999 Water exchange reactions and hydrolysis of hydrated Titanium(III) ions. A density functional theory study. *J. Phys. Chem. A* **103**, 9899–9905. (doi:10.1021/jp9918508)
- Haumann, M. & Junge, W. 1999 Evidence for impaired hydrogen-bonding of tyrosine  $Y_Z$  in calcium-depleted photosystem II. *Biochim. Biophys. Acta* **1411**, 121–133. (doi:10.1016/S0005-2728(99)00045-6)
- Helm, L. & Merbach, A. E. 1999 Water exchange on metal ions: experiments and simulations. *Coord. Chem. Rev.* **187**, 151–181. (doi:10.1016/S0010-8545(99)90232-1)
- Hendry, G. & Wydrzynski, T. 2003  $^{18}\text{O}$  isotope exchange measurements reveal that calcium is involved in the binding of one substrate-water molecule to the oxygen-evolving complex in photosystem II. *Biochemistry* **42**, 6209–6217. (doi:10.1021/bi034279i)
- Hillier, W. & Wydrzynski, T. 2000 The affinities for the two substrate water binding sites in the  $\text{O}_2$  evolving complex of photosystem II vary independently during S-state turnover. *Biochemistry* **39**, 4399–4405. (doi:10.1021/bi992318d)
- Hillier, W. & Wydrzynski, T. 2001 Oxygen ligand exchange at metal sites—implications for the  $\text{O}_2$  evolving mechanism of photosystem II. *Biochim. Biophys. Acta: Bioenerg.* **1503**, 197–209. (doi:10.1016/S0005-2728(00)00225-5)
- Hillier, W. & Wydrzynski, T. 2004 Substrate water interactions within the photosystem II oxygen evolving complex. *Phys. Chem. Chem. Phys.* **6**, 4882–4889. (doi:10.1039/b407269c)
- Hoganson, C. W. & Babcock, G. T. 1997 A metalloradical mechanism for the generation of oxygen from water in photosynthesis. *Science* **277**, 1953–1956. (doi:10.1126/science.277.5334.1953)
- Houston, J. R., Richens, D. T. & Casey, W. H. 2006 Distinct water-exchange mechanisms for trinuclear transition-metal clusters. *Inorg. Chem.* **45**, 7962–7967. (doi:10.1021/ic0609608)
- Iuzzolino, L., Dittmer, J., Dorner, W., Meyer-Klaucke, W. & Dau, H. 1998 X-ray absorption spectroscopy on layered photosystem II membrane particles suggests manganese-centered oxidation of the oxygen-evolving complex for the  $\text{S}_0$ – $\text{S}_1$ ,  $\text{S}_1$ – $\text{S}_2$ , and  $\text{S}_2$ – $\text{S}_3$  transitions of the water oxidation cycle. *Biochemistry* **37**, 17 112–17 119. (doi:10.1021/bi9817360)
- Joliot, P. J., Trost, J. T. & Diner, B. A. 1969 A new model of photochemical centers in system-2. *Photochem. Photobiol.* **10**, 309–329.
- Kimura, Y., Mizusawa, N., Yamanari, T., Ishii, A. & Ono, T. 2005 Structural changes of D1 C-terminal  $\alpha$ -carboxylate during S-state cycling in photosynthetic oxygen evolution. *J. Biol. Chem.* **280**, 2078–2083. (doi:10.1074/jbc.M410627200)
- Kok, B., Forbush, B. & McGloin, M. 1970 Cooperation of charges in photosynthetic  $\text{O}_2$  evolution—I. A linear four step mechanism. *Photochem. Photobiol.* **11**, 457–475.
- Kuzek, D. & Pace, R. J. 2001 Probing the Mn oxidation states in the OEC. Insights from spectroscopic, computational and kinetic data. *Biochim. Biophys. Acta* **1503**, 123–137. (doi:10.1016/S0005-2728(00)00218-8)
- Lundberg, M., Blomberg, M. R. A. & Siegbahn, P. E. M. 2003 Modeling water exchange on mono- and dimeric Mn-centers. *Theor. Chem. Acc.* **110**, 130–143.
- McEvoy, J. P. & Brudvig, G. W. 2004 Structure-based mechanism of photosynthetic water oxidation. *Phys. Chem. Chem. Phys.* **6**, 4754–4763. (doi:10.1039/b407500e)
- McEvoy, J. P., Gascon, J. A., Batista, V. B. & Brudvig, G. 2005a Computational structural model of the oxygen evolving complex in photosystem II: complete ligation by protein, water and chloride. In *Photosynthesis: fundamental aspects to global perspectives*, vol. 1 (eds D. Bruce & A. van der Est), pp. 278–280. Lawrence, KA: Allen Press, Inc.
- McEvoy, J. P., Gascon, J. A., Batista, V. B. & Brudvig, G. 2005b The mechanism of photosynthetic water splitting. *Photochem. Photobiol. Sci.* **4**, 940–949. (doi:10.1039/b506755c)
- Messinger, J. 2004 Evaluation of different mechanistic proposals for water oxidation in photosynthesis on the basis of  $\text{Mn}_4\text{O}_x\text{Ca}$  structures for the catalytic site and spectroscopic data. *Phys. Chem. Chem. Phys.* **6**, 4764–4771. (doi:10.1039/b406437b)
- Messinger, J. et al. 2001 Absence of Mn-centered oxidation in the  $\text{S}_2 \rightarrow \text{S}_3$  transition: implications for the mechanism of photosynthetic water oxidation. *J. Am. Chem. Soc.* **123**, 7804–7820. (doi:10.1021/ja004307+)
- Noguchi, T. & Sugiura, M. 2002 FTIR detection of water reactions during the flash-induced S-state cycle of the photosynthetic water-oxidizing complex. *Biochemistry* **41**, 15 706–15 712. (doi:10.1021/bi020603i)
- Nugent, J. H. A., Rich, A. M. & Evans, M. C. W. 2001 Photosynthetic water oxidation: towards a mechanism. *Biochim. Biophys. Acta* **1503**, 138–146. (doi:10.1016/S0005-2728(00)00223-1)
- Ono, T., Noguchi, T., Inoue, Y., Kusunoki, M., Matsushita, T. & Oyanagi, H. 1992 X-ray detection of the period-four cycling of the manganese cluster in photosynthetic water oxidizing enzyme. *Science* **258**, 1335–1337. (doi:10.1126/science.258.5086.1335)
- Pecoraro, V. L., Baldwin, M. J. & Gelasco, A. 1994 Interaction of manganese with dioxygen and its reduced derivatives. *Chem. Rev.* **94**, 807–826. (doi:10.1021/cr00027a012)
- Pecoraro, V. L., Baldwin, M. J., Caudle, M. T., Hsieh, W. Y. & Law, N. A. 1998 A proposal for water oxidation in photosystem II. *Pure Appl. Chem.* **70**, 925–929.

- Reed, A. E., Curtiss, L. A. & Weinhold, F. 1988 Inter-molecular interactions from a natural bond orbital, donor-acceptor viewpoint. *Chem. Rev.* **88**, 899–926. (doi:10.1021/cr00088a005)
- Robblee, J. H., Cinco, R. M. & Yachandra, V. K. 2001 X-ray spectroscopy based structure of the Mn cluster and mechanism of photosynthetic oxygen evolution. *Biochim. Biophys. Acta* **1503**, 7–23. (doi:10.1016/S0005-2728(00)00217-6)
- Roelofs, T. A., Liang, W. C., Latimer, M. J., Cinco, R. M., Rompel, A., Andrews, J. C., Sauer, K., Yachandra, V. K. & Klein, M. P. 1996 Oxidation states of the manganese cluster during the flash-induced S-state cycle of the photosynthetic oxygen-evolving complex. *Proc. Natl Acad. Sci. USA* **93**, 3335–3340. (doi:10.1073/pnas.93.8.3335)
- Rotzinger, F. P. 1997 Mechanism of water exchange for the di- and trivalent metal hexaaqua ions of the first transition series. *J. Am. Chem. Soc.* **119**, 5230–5238. (doi:10.1021/ja9635950)
- Rotzinger, F. P. 2005 Performance of molecular orbital methods and density functional theory in the computation of geometries and energies of metal aqua ions. *J. Phys. Chem. B* **109**, 1510–1527. (doi:10.1021/jp045407v)
- Schlodder, E. & Witt, H. T. 1999 Stoichiometry of proton release from the catalytic center in photosynthetic water oxidation. *J. Biol. Chem.* **274**, 30 387–30 392. (doi:10.1074/jbc.274.43.30387)
- Schrodinger, L. 2004 *JAGUAR 5.5*. Portland, Oregon: Schrodinger, Inc.
- Sproviero, E. M., Gascon, J. A., McEvoy, J. P., Brudvig, G. W. & Batista, V. S. 2006a QM/MM models of the O<sub>2</sub>-evolving complex of photosystem II. *J. Chem. Theor. Comput.* **2**, 1119–1134. (doi:10.1021/ct060018l)
- Sproviero, E. M., Gascon, J. A., McEvoy, J. P., Brudvig, G. W. & Batista, V. S. 2006b Characterization of synthetic oxomanganese complexes and the inorganic core of the O<sub>2</sub>-evolving complex in photosystem II: evaluation of the DFT/B3LYP level of theory. *J. Inorg. Biochem.* **100**, 786–800. (doi:10.1016/j.jinorgbio.2006.01.017)
- Sproviero, E. M., Gascon, J. A., McEvoy, J. P., Brudvig, G. W. & Batista, V. S. 2007 Quantum mechanics/molecular mechanics structural models of the oxygen-evolving complex of photosystem II. *Curr. Opin. Struct. Biol.* **17**, 173–180. (doi:10.1016/j.sbi.2007.03.015)
- Tagore, R., Chen, H. Y., Crabtree, R. H. & Brudvig, G. W. 2006 Determination of  $\mu$ -oxo exchange rates in di- $\mu$ -oxo dimanganese complexes by electrospray ionization mass spectrometry. *J. Am. Chem. Soc.* **128**, 9457–9465. (doi:10.1021/ja061348i)
- Tagore, R., Crabtree, R. H. & Brudvig, G. W. 2007 Distinct mechanisms of bridging-oxo exchange in di- $\mu$ -O dimanganese complexes with and without water-binding sites: implications for water binding in the O<sub>2</sub>-evolving complex of photosystem II. *Inorg. Chem.* **46**, 2193–2203. (doi:10.1021/ic061968k)
- Tsutsui, Y., Wasada, H. & Funahashi, S. 1999 Reaction mechanism of water exchange on di- and trivalent cations of the first transition series and structural stability of seven-coordinate species. *THEOCHEM* **461–462**, 379–390. (doi:10.1016/S0166-1280(98)00451-5)
- Vacek, G., Perry, J. K. & Langlois, J. M. 1999 Advanced initial-guess algorithm for self-consistent-field calculations on organometallic systems. *Chem. Phys. Lett.* **310**, 189–194. (doi:10.1016/S0009-2614(99)00722-8)
- Vallet, V., Wahlgren, U., Schimmelpennig, B., Szabo, Z. & Grenthe, I. 2001 The mechanism for water exchange in [UO<sub>2</sub>(H<sub>2</sub>O)<sub>5</sub>]<sup>2+</sup> and [UO<sub>2</sub>(oxalate)<sub>2</sub>(H<sub>2</sub>O)]<sup>2-</sup>, as studied by quantum chemical methods. *J. Am. Chem. Soc.* **123**, 11 999–12 008. (doi:10.1021/ja015935+)
- Vrettos, J. S., Limburg, J. & Brudvig, G. W. 2001 Mechanism of photosynthetic water oxidation: combining biophysical studies of photosystem II with inorganic model chemistry. *Biochim. Biophys. Acta* **1503**, 229–245. (doi:10.1016/S0005-2728(00)00214-0)
- Yachandra, V. K., DeRose, V. J., Latimer, M. J., Mukerji, I., Sauer, K. & Klein, M. P. 1993 Where plants make oxygen: a structural model for the photosynthetic oxygen-evolving manganese cluster. *Science* **260**, 675–679. (doi:10.1126/science.8480177)
- Yachandra, V. K., Sauer, K. & Klein, M. P. 1996 Manganese cluster in photosynthesis: where plants oxidize water to dioxygen. *Chem. Rev.* **96**, 2927–2950. (doi:10.1021/cr950052k)
- Zheng, M. & Dismukes, G. C. 1996 Orbital configuration of the valence electrons, ligand field symmetry, and manganese oxidation states of the photosynthetic water oxidizing complex: analysis of the S<sub>2</sub> state multiline EPR signals. *Inorg. Chem.* **35**, 3307–3319. (doi:10.1021/ic9512340)

### Discussion

V. L. Pecoraro (*University of Michigan, Michigan, USA*). How did you truncate the protein to do your calculations?

V. S. Batista. The models consider about 2000 atoms of PSII including the Mn<sub>3</sub>CaO<sub>4</sub>Mn complex and all amino acid residues with  $\alpha$ -carbons within 15 Å from any atom in the OEC metal cluster.

V. L. Pecoraro. How did you determine the boundary between QM and MM regions?

V. S. Batista. Determining the QM/MM boundary requires an iterative approach where the structural and electronic (spin-state) properties of the system are evaluated for various different sizes of the QM layer. The QM/MM boundary is defined for subsequent calculations so that results are converged relative to the size of the QM layer.

V. L. Pecoraro. How did you determine the coordination number of Ca<sup>2+</sup>?

V. S. Batista. We obtained fully relaxed configurations of the system and we counted the number of ligands in the first coordination sphere with distances smaller than approximately 3 Å from Ca<sup>2+</sup>.

W. L. Junge (*University of Osnabrück, Osnabrück, Germany*). What was the calculated relaxation time of your calculations?

V. S. Batista. We have analysed only stationary states.

W. L. Junge. Concerning the hydrophobic environment of chloride, what would be the effective dielectric constant?

V. S. Batista. The dielectric constant of the surrounding protein environment is estimated to be approximately 4.

P. E. M. Siegbahn (*Stockholm University AlbaNova University Center, Stockholm Center for Physics, Astronomy and Biotechnology, Stockholm, Sweden*). In your talk, you focused on strong-field, low-spin states. In the OEC chemistry, it is probably quite important that the ground states are weak-field, high-spin states. Have you, or are you intending to do work with high-spin states?

V. S. Batista. We have explored the relative stability of high-spin versus low-spin states in various benchmark complexes previously characterized by EPR and X-ray spectroscopic measurements. In addition, we have performed an exhaustive analysis of relaxed conformations of the OEC in various possible initial-guess spin-electronic states.